One-Dimensional Centrifugation Model

Steven H. Chan, San Kiang, and Matthew A. Brown
Process Research and Development, Bristol-Myers Squibb Pharmaceutical Research Institute, Engineering Technology Dept., New Brunswick, NJ 08903

A 1-D theoretical model based on Darcy's law and conservation of mass was used to describe transient filtration on a basket centrifuge for both compressible and incompressible cakes. This filtration model was validated assuming that a liquid layer lay above the surface of the cake. Both the resistance and porosity of the cake were assumed constant throughout the cake at a particular instant in time. A computational algorithm was developed to solve the system of nonlinear equations and to calculate pressure differentials across the cake, location of the slurry front in the basket, cake thickness, filtrate volume, cake resistance, cake porosity, and filtrate flow rate, all as functions of time. Both simulation and experimental results showed the validity of this computational model. A procedure was also developed to use small-scale lab data, in conjunction with the model, to select the corresponding operating conditions for large-scale equipment so that cake performance on both scales was dynamically similar. For the situation when the inlet feed had ceased and the liquid layer had fallen below the surface of the cake, the cake deliquoring model proposed by Wakeman and Vince was adopted.

Introduction

Solid/liquid separation is a very important unit operation in the pharmaceutical industry, because in the majority of the cases, our desired product is generally a high-purity solid in its final form. The filtration performance for the crystal slurry is largely dependent on the past history of the feed solution. Changes in the crystallization conditions can often alter the size distribution or the shape of the particles. In addition to the normal cycle time, the integrity of the solid particles and the washability of the cake are very important for product quality.

A review of the literature shows that a transient model incorporating both centrifugal sedimentation and centrifugal filtration has been proposed by Sambuichi et al. (1987) to describe the solid/liquid separation at relatively low acceleration (75–300 g). The centrifugation experiments consist of delivering a known slurry volume in one portion, and the decrease in the liquid layer during drainage is monitored using stroboscopic photography. In Sambuichi et al.'s work the flow rate of the inlet slurry to the centrifuge is not a parameter in their model and the maximum cake deposited on the centrifuge is 5 mm (6% of the centrifuge radius). In industrial applications the inlet feed rate is a very important parameter to be considered especially in a theoretical model. In their work both the resistance and the porosity of the cake are assumed to exhibit constant values when the compressive pressure is below a critical value.

Wakeman (1994) has also presented a model for cake formation and growth in basket centrifuges. This model accounts for the simultaneous sedimentation and filtration, and also includes the relative effects of each mechanism in their contribution to cake development. The cake permeability and porosity are used as curve-fitting parameters, to obtain good agreement between the experimental and calculated solids deposited. Difficulties in measuring the centrifuge cake thickness while the basket is spinning can lead to uncertainties in the determination of these parameters. In Wakeman's work, a plot of the filtrate flow rate vs. time shows that the general shape of the curve is exhibited by both theory and experiment, but there are deviations in their exact values.

In the work of Tiller and Hsyung (1991), a more advanced mathematical model is presented considering the two-dimensional (2-D) nature of a compressible cake during filtration in a centrifuge. The analysis is confined to theoretical conditions existing in cakes at equilibrium. In their investigation, absent from consideration are transient times, effect of the

Correspondence concerning this article should be addressed to S. H. Chan.

conveying mechanism in sedimenting centrifuges, and drainage after cake formation in filtering centrifuges.

In this article, a 1-D theoretical model based on Darcy's law and conservation of mass is used to predict the filtration performance on a centrifuge for both compressible and incompressible cakes. This model is valid when the liquid lies above the surface of the cake. The model provides a critical test of the processing conditions on a small scale. It allows for the selection of an optimum performance condition (such as angular rotation speed, inlet flow rate, and so on) from among a number of alternatives without performing numerous experiments.

This filtration model is developed to describe the physical problem and is used as a tool to make reliable scale-up predictions based on small-scale lab experiments. As a consequence of the model, the same dynamic performance on two different scales is predicted as long as the following relationship $\omega_1 r_1 = \omega_2 r_2$ holds.

In this investigation, no experimental deliquoring data are collected on the centrifuge. However, the deliquoring model proposed by Wakeman and Vince (1986) is adopted in this study. It is valid when the inlet feed has stopped and the liquid falls below the surface of the cake. Estimates of the threshold saturation and the minimum pressure needed to displace the liquid held by capillary forces in the model are obtained using empirical relationships published in the filtration literature. Both the 1-D filtration model and the deliquoring model are incorporated in this article to completely describe the overall solid liquid separation process.

Experimentally, leaf filter tests performed at one constant pressure do not provide sufficient information to predict and to extrapolate the filtration performance on a basket centrifuge. In fact, multiple leaf filter experiments at different pressures are necessary to arrive at empirical relationships that can relate both the resistance and the porosity of the cake as functions of the compressive pressure.

A 1-D centrifugation model for solid/liquid separation is presented in this article. The slurry is assumed to be dense and very fast settling, so the presence of a slurry layer is absent in the basket. It is assumed that the liquid layer lies above the surface of the cake. The cake deliquoring model is adopted for the case when the inlet feed is zero and the liquid lies below the surface of the cake. In this article, experiments are performed on an organic entity, referred to as "Compound A", due to the proprietary nature of the solid to be investigated. Experiments performed on a basket centrifuge for the filtration process are then compared with our theoretical model. For the deliquoration of the cake, only simulation results are presented.

Formulation of the Filtration Model

Figure 1 shows a horizontal basket centrifuge used in the formulation of the mathematical model. In a basket centrifuge with radius r_0 the hydraulic pressure Δp is related to the radius of the liquid layer r_ℓ by the following equation

$$\Delta p = \frac{\rho_\ell \omega^2}{2}\left(r_0^2 - r_\ell^2\right) \tag{1}$$

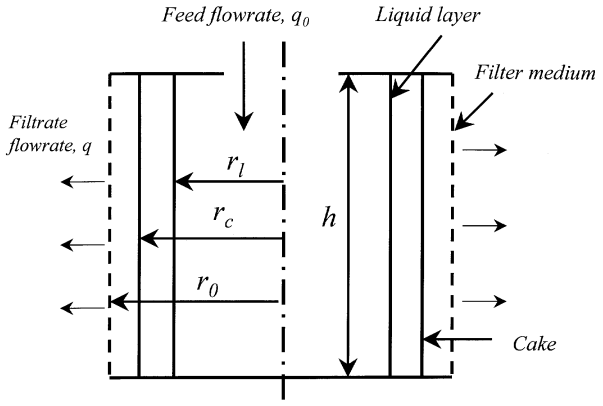

Figure 1. Horizontal basket centrifuge.

where ρ_ℓ is the density of the filtrate and ω is the angular velocity of the centrifuge basket. This relationship shows that the hydraulic pressure can be increased either by decreasing the value of r_l or by increasing the angular velocity.

According to Sambuichi et al. (1987), the following relationship, derived from Darcy's law, is used to predict the prediction of the filtration performance in a centrifuge

$$q = \frac{dV}{dt} = \frac{\Delta p}{\dfrac{\alpha_{av}\mu c V}{A_{av}A_{lm}} + \dfrac{\mu R_m}{A_0}} \tag{2}$$

The volumetric flow rate of the filtrate q is directly proportional to the hydraulic pressure and is inversely proportional to the sum of both the cake resistance α_{av} and the medium resistance R_m. In the above relationship, μ is the kinematic viscosity of the filtrate, c is the mass of the dry solids divided by the filtrate volume collected, and V is the volume of filtrate collected. A_{lm}, A_{av}, and A_0 are the logarithmic mean area of the flow, the arithmetic mean flow area in the cake, and the medium area, respectively, and are defined as follows

$$A_{lm} = \frac{2\pi h(r_0 - r_c)}{\ln(r_0/r_c)} \tag{3}$$

$$A_{av} = \frac{2\pi h(r_0 + r_c)}{2} \tag{4}$$

$$A_0 = 2\pi r_0 h \tag{5}$$

where h is the height of the centrifuge and r_c is the distance from the center to the surface of the cake.

An overall solid balance at time t that relates the cake radius to the inlet feed rate may be written by equating the solids in the feed to the solids deposited on the filter

$$q_0 t V_s = \pi(1 - \epsilon_{av})\left(r_0^2 - r_c^2\right)h \tag{6}$$

where V_s is the solid volume fraction of the inlet feed, q_0 is the inlet feed rate, and ϵ_{av} is the average porosity in the cake. This expression assumes the absence of a slurry layer

above the cake. Once the slurry is deposited on the basket, it is assumed that the formation of both a cake and a liquid layer is instantaneous. In reality, a porosity distribution occurs across the cake. This distribution can be considered in a 2-D model. In this 1-D model, the porosity is assumed to be constant everywhere in the cake at any particular instant in time.

Because filtration is a transient process, the porosity and the cake radius are changing as functions of time. Differentiation of Eq. 6 with respect to time gives

$$q_0 V_s = -\pi\left(r_0^2 - r_c^2\right)h\frac{d\epsilon_{av}}{dt} - 2\pi r_c(1-\epsilon_{av})h\frac{dr_c}{dt} \quad (7)$$

Because of the assumption of a very fast settling slurry, a liquid layer lies above the surface of the cake ($r_c \le r_\ell$). An overall liquid balance written for this case is

$$tq_0(1-V_s) - V = \pi\epsilon_{av}\left(r_0^2 - r_c^2\right)h + \pi\left(r_\ell^2 - r_c^2\right)h \quad (8)$$

Differentiation of Eq. 8 with respect to time yields

$$q_0(1-V_s) - \frac{dV}{dt} = \pi h\left(r_0^2 - r_c^2\right)\frac{d\epsilon_{av}}{dt} - 2\pi\epsilon_{av}hr_c\frac{dr_c}{dt} + \pi h\left(2r_\ell\frac{dr_\ell}{dt} - 2r_c\frac{dr_c}{dt}\right) \quad (9)$$

Even when the inlet feed has stopped during the filtration process, the above relationship is valid provided that a liquid layer lies above the surface of the cake. For the situation when $q_0 = 0$ and the liquid layer falls below the surface of the cake ($r_\ell \le r_c$), a different mathematical formulation for cake deliquoring is discussed in the subsequent section.

The power law constitutive relationships, shown below, are used extensively in the filtration literature (Sambuichi et al., 1987; Wakeman and Tarleton, 1999; Lu et al., 1998; Tiller and Leu, 1980)

$$\alpha_{av} = \alpha_0(\Delta p_s)^{n_1} \quad (10)$$

and

$$\epsilon_{av} = \epsilon_0(\Delta p_s)^{-n_2} \quad (11)$$

where α_{av} is the average cake resistance, ϵ_{av} is the average cake porosity, (Δp_s) is the compressive pressure of the cake, and α_0, ϵ_0, n_1, and n_2 and constants. Relationships 10 and 11 are limited to large Δp_s. Fournet et al. (1992) have determined the values of α_0 and n_1 for both glass beads and salicylic acid crystals using a cylindrical filter cell and a basket centrifuge with a pre-deposited thickness of cake. A comparison of the experimental parameters obtained using these equipment yield values that are correct to within 15%. In this article, the values of α_0 and n_1 are determined by performing leaf filter experiments similar to the analysis used by Fournet et al. (1992). These experimentally determined values were then used to predict the filtration performance in a centrifuge. In this model, the compressive pressure is defined as

$$\Delta p_s = \frac{\rho_\ell\omega^2}{2}\left(r_0^2 - r_c^2\right) \quad (12)$$

which is the expression derived originally by Tiller and Hsyung (1991).

Cake Deliquoring Model ($r_\ell \le r_c$)

The centrifuge deliquoring process, when $q_0 = 0$ and liquid layer falls below the surface of the cake ($r_\ell \le r_c$), can be described by the equation derived by Wakeman and Vince (1986)

$$\frac{\partial S}{\partial t} = \frac{-k}{\epsilon_{av}\mu}\left[k_{r\ell}\left(\rho_\ell\omega^2 - \frac{\partial^2 p_c}{dr^2}\right) + \left(\rho_\ell\omega^2 r - \frac{\partial p_c}{\partial r}\right)\left(\frac{\partial k_{r\ell}}{\partial r} + \frac{k_{r\ell}}{r}\right)\right] \quad (13)$$

where p_c is the capillary pressure, S is the cake saturation, $k_{r\ell}$ is the relative permeability of the cake to the liquid phase, and k is the permeability of the saturated medium. This treatment assumes the bed is considered as an homogeneous network of voids (constant porosity distribution), which are initially saturated with a liquid. The cake saturation S is defined as

$$S = \frac{V_\ell}{V_{\text{pore}}} \quad (14)$$

where V_ℓ is the liquid volume in the cake and V_{pore} is the void volume in the cake. k is related to the saturated resistance of the cake by

$$k = \frac{1}{k_{r\ell}\rho_t(1-\epsilon_{av})\alpha_{av}} \quad (15)$$

where ρ_t is the true density of the powder. The relative permeability of the liquid phase $k_{r\ell}$ is

$$k_{r\ell} = S_R^{(2+\lambda)/\lambda} \quad (16)$$

where λ is the pores size index which characterizes the range of pore sizes in the filter cake and S_R is the reduced saturation.

The reduced saturation S_R is defined by

$$S_R = \frac{S - S_\infty}{1 - S_\infty} \quad (17)$$

so that

$$\frac{\partial S}{\partial t} = \left[(1-S_R)\frac{\partial S_\infty/\partial r}{\partial S_R/\partial r} + (1-S_\infty)\right]\frac{\partial S_R}{\partial t} \quad (18)$$

where S_∞ is the saturation at which liquid flow ceases. When $S \le S_\infty$, no more liquid can be removed from the cake by the deliquoring process except through evaporative or drying techniques. An empirical relationship correlating the reduced saturation with the capillary pressure is described by Wakeman (1976)

$$S_R = \left(\frac{p_b}{p_c}\right)^{\lambda} \tag{19}$$

where p_b is the minimum pressure needed to initiate displacement of liquid. An estimate for the value of p_b can be obtained by the relationship (Wakeman, 1976) below

$$p_b = \frac{4.6(1-\epsilon_{av})\sigma}{\epsilon_{av} x} \tag{20}$$

where σ is the liquid surface tension and x is the mean particle size. Empirical correlations for the irreducible saturation of centrifuge cakes are represented by the equations of Wakeman and Rushton (1977)

$$\begin{aligned} S_\infty &= 0.0524 N_{\text{cap}}^{-0.19} \qquad \text{for } 10^{-5} \le N_{\text{cap}} \le 0.14 \\ &= 0.0139 N_{\text{cap}}^{-0.86} \qquad \text{for } 0.14 \le N_{\text{cap}} \le 10 \end{aligned} \tag{21}$$

where the capillary number N_{cap} is defined as

$$N_{cap} = \frac{\epsilon_{av} x^2 \rho_\ell \omega^2 r}{(1-\epsilon_{av})^2 \sigma} \tag{22}$$

The average reduced saturation is calculated by

$$S_{R,\text{avg}} = \frac{\int_{r_c}^{r_0} S_R 2\pi r h \, dr}{\int_{r_c}^{r_0} 2\pi r h \, dr} \tag{23}$$

Substitution of Eqns. 16, 18, and 19 into Eq. 13 yields

$$\begin{aligned} \frac{\partial S_R}{\partial t}\left[(1-S_R)\frac{\partial S_\infty/\partial r}{\partial S_R/\partial r} + (1-S_\infty)\right]\frac{\epsilon_{av}\mu}{k} &= \rho_\ell \omega^2 S_R^{(2+\lambda)/\lambda} \\ &+ \frac{p_b}{\lambda}\left[S_R^{1/\lambda}\frac{\partial^2 S_R}{\partial r^2} - \left(\frac{1+\lambda}{\lambda}\right)S_R^{(1-\lambda)/\lambda}\left(\frac{\partial S_R}{\partial r}\right)^2\right] \\ &+ \left[\rho_\ell \omega^2 r + \frac{p_b}{\lambda} S_R^{-(1+\lambda)/\lambda}\frac{\partial S_R}{\partial r}\right] \\ &\times \left[\left(\frac{2+3\lambda}{\lambda}\right)S_R^{(2+2\lambda)/\lambda}\frac{\partial S_R}{\partial x} + \frac{S_R^{(2+3\lambda)/\lambda}}{r}\right] \end{aligned} \tag{24}$$

By introducing the following dimensionless variables

$$r^* = \frac{r}{r_0} \tag{25}$$

$$r_1^* = \frac{r_c}{r_0} \tag{26}$$

$$t^* = \frac{k p_b t}{\mu r_0^2 \epsilon_{av}(1-S_\infty)} \tag{27}$$

$$t_s^* = \frac{k p_b t_s}{\mu r_0^2 \epsilon_{av}(1-S_\infty)} \tag{28}$$

where t_s is the instant when the liquid layer falls to the same level as the surface of the cake, Eq. 24 transforms into

$$\begin{aligned} \frac{\partial S_R}{\partial t^*} &= 2A_1 S_R^{(2+3\lambda)/\lambda} + \left(A_2 r^* S_R^{2(1+\lambda)/\lambda} + \frac{A_3}{r^*} S_R^{2(1+\lambda)/\lambda}\right) \\ &\frac{\partial S_R}{\partial r^*} + A_4 S_R^{(1+\lambda)/\lambda}\left(\frac{\partial S_R}{\partial r^*}\right)^2 + A_3 S_R^{(1+2\lambda)/\lambda}\frac{\partial^2 S_R}{\partial r^{*2}} \end{aligned} \tag{29}$$

where

$$A_1 = -\frac{\rho_\ell \omega^2 r_0^2}{p_b} \tag{30}$$

$$A_2 = \frac{2+3\lambda}{\lambda} A_1 \tag{31}$$

$$A_3 = -\frac{1}{\lambda} \tag{32}$$

$$A_4 = -\frac{1+2\lambda}{\lambda^2} \tag{33}$$

subject to the following initial and boundary conditions

$$t^* = t_s^* \qquad S_R = 1 \qquad r_1^* \le r^* \le 1 \tag{34}$$

$$t^* > t_s^* \qquad S_R = 0 \qquad r^* = r_1^*$$

$$\frac{\partial S_R}{\partial r^*} = 0 \qquad r^* = 1 \tag{35}$$

The volume of liquid displaced from the cake during deliquoring is calculated by

$$V_\ell|_{t=t_f} - V_\ell|_{t=t_s} = \left(S|_{t=t_f} - S|_{t=t_s}\right)V_{\text{pore}} \tag{36}$$

where $V_\ell|_{t=t_f}$ is the liquid volume in the cake at time t_f, $V|_{t=t_s}$ is the liquid volume when the cake is fully saturated at time t_s, $S|_{t=t_f}$ is the cake saturation at time t_f, and $S|_{t=t_s}$ is the cake saturation when the cake is completely saturated at time t_s. The instantaneous filtrate flow rate is calculated by

$$q = \frac{-dV_\ell}{dt} = -V_{\text{pore}}\frac{dS}{dt} \tag{37}$$

Solution Methodology for Filtration Model

Before solving the system of highly coupled nonlinear differential equations, it is assumed that both the cake resistance and the porosity can be expressed as functions of the compressive pressure. The determination of these constants in the constitutive equations is discussed in the experimental section of this article. Other physical parameters such as ρ_ℓ, μ, r_0, h, and V_s must also be known *a priori* either through

physical measurements or from known literature values. For a given centrifuge geometry with a fixed slurry concentration, the inlet feed rate and the angular velocity of the centrifuge are two physical parameters that can be varied.

The logarithmic mean area, the arithmetic mean flow area, and the medium flow area, defined in Eqs. 3–5, are substituted into Eq. 2. After substitution, Eq. 2 is expressed implicitly as a function of the following variables

$$f_1\left(\Delta p,\ \alpha_{av}, V, r_c, \frac{dV}{dt}\right) = 0 \tag{38}$$

Corresponding to Eqs. 1, 7, 9, 10, 11, and 12, their respective functions can be similarly expressed implicitly as follows

$$f_2(\Delta p, r_\ell) = 0 \tag{39}$$

$$f_3\left(r_c, r_\ell, \frac{d\epsilon_{av}}{dt}, \frac{dr_c}{dt}\right) = 0 \tag{40}$$

if $r_c \le r_\ell$, then

$$f_{4a}\left(r_c, \frac{dV}{dt}, \frac{d\epsilon_{av}}{dt}, \frac{dr_c}{dt}, \frac{dr_\ell}{dt}\right) = 0 \tag{41}$$

$$f_5(\alpha_{av}, \Delta p_s) = 0 \tag{42}$$

$$f_6(\epsilon_{av}, \Delta p_s) = 0 \tag{43}$$

$$f_7(\Delta p_s, r_c) = 0 \tag{44}$$

This present model also allows for the input feed flow to be stopped at any instant during the process by setting $q_0 = 0$ under the condition that the liquid layer lies above the surface of the cake.

Since there are seven independent equations, there must be a total of seven unknown variables in order for the problem to be consistent. These seven variables include Δp, Δp_s, r_c, r_ℓ, V, ϵ_{av}, and α_{av}. The system of nonlinear equations, consisting of Eqs. 39–44, is linearized (Chan and Cheh, 2001) and is solved numerically using the method of finite differences (Gerald and Wheatly, 1994). Similar to the mathematical treatment of the constitutive equations by Sambuichi et al. (1987), both the resistance and the porosity of the cake are assumed to exhibit constant values when the compressive pressure is below a minimum compressive pressure $\Delta p_{s,0}$

$$\alpha_{av} = \alpha_0(\Delta p_{s,0})^{n_1} \quad \text{when } \Delta p_s < \Delta p_{s,0} \tag{45a}$$

$$\alpha_{av} = \alpha_0(\Delta p_s)^{n_1} \quad \text{when } \Delta p_s > \Delta p_{s,0} \tag{45b}$$

$$\epsilon_{av} = \epsilon_0(\Delta p_{s,0})^{-n_2} \quad \text{when } \Delta p_s < \Delta p_{s,0} \tag{46a}$$

$$\epsilon_{av} = \epsilon_0(\Delta p_s)^{-n_2} \quad \text{when } \Delta p_s > \Delta p_{s,0} \tag{46b}$$

With this treatment, the system of equations is then subjected to the initial boundary conditions ($t = 0$)

$$\Delta p = 0 \tag{47a}$$

$$\Delta p_s = 0 \tag{47b}$$

$$r_c = r_0 \tag{47c}$$

$$r_\ell = r_0 \tag{47d}$$

$$V = 0 \tag{47e}$$

$$\epsilon_{av} = \epsilon_0(\Delta p_{s,0})^{-n_2} \tag{47f}$$

and

$$\alpha_{av} = \alpha_0(\Delta p_{s,0})^{n_1} \tag{47g}$$

The input information for the solution algorithm includes: the angular velocity ω, the dimensions of the centrifuge and r and h, the inlet feed rate q_0, the time to stop inlet feed rate t_{stop}, and the end time for the filtration process t_{end}. For the first time increment ($t = \Delta t$), the solution for these seven equations at the first iteration is solved by making initial guesses for the seven variables denoted by $\Delta p_i^{\text{guess}}$, $\Delta p_{s,i}^{\text{guess}}$, $r_{c,i}^{\text{guess}}$, $r_{\ell,i}^{\text{guess}}$, V_i^{guess}, $\epsilon_{av,i}^{\text{guess}}$, and $\alpha_{av,i}^{\text{guess}}$ to be equal to the initial boundary conditions. After the first iteration, the updated values from solving these seven simultaneous equations yield $\Delta p_i^{\text{updated}}$, $\Delta p_{s,i}^{\text{updated}}$, $r_{c,i}^{\text{updated}}$, $r_{\ell,i}^{\text{updated}}$, V_i^{updated}, $\epsilon_{av,i}^{\text{updated}}$, and $\alpha_{av,i}^{\text{updated}}$. If the absolute difference between the updated and the guess values is greater than an error tolerance of 10^{-8}, then the guess values are replaced with the updated values. The iterative process is repeated again until the error tolerance is met. Once the criterion for the set tolerance is satisfied, the solution has converged for that particular time step and the time is incremented again by Δt. If the new time exceeds or equals t_{stop}, the inlet feed rate is set to zero. If the new time exceeds or equals t_{end}, no more calculations are performed and the numerical algorithm stops here. The same iterative process is repeated again for the next time step. Thereafter, the solution at the subsequent time step is solved by letting the guess values equal to the converged values from the previous time step. A block diagram, shown in Figure 2, summarizes the iterative algorithm used to solve the system of nonlinear differential equations.

By running a series of simulations at various time steps, the optimum time step is determined by taking a maximum value of Δt where there is no change in the plot of the filtrate volume vs. time for decreasing values of Δt. The optimum time step is determined to be 0.05 s. All of the simulations presented here are performed using a time increment of 0.0125 s, which is one-fourth of the optimum value.

Solution Methodology for Cake Deliquoring Model

The average cake porosity ϵ_{av} is calculated using the centrifuge filtration model when the liquid layer is equal to the cake layer ($r_c = r_\ell$). It is assumed that, when the liquid layer falls below the surface of the cake, the average porosity remains constant throughout the deliquoring process. p_b, the minimum pressure needed to initiate displacement of liquid inside the capillary, is estimated by Eq. 20. In the absence of the experimental cake deliquoring data, the threshold saturation S_∞ can be estimated from the empirical relationships given in both Eqs. 21 and 22. According to Wakeman (Wakeman and Tarleton, 1999), a reasonable value for λ, the pore size index, is suggested to be 5.

The start time t_s for the deliquoring model continues from the end time of the filtration model and occurs when the

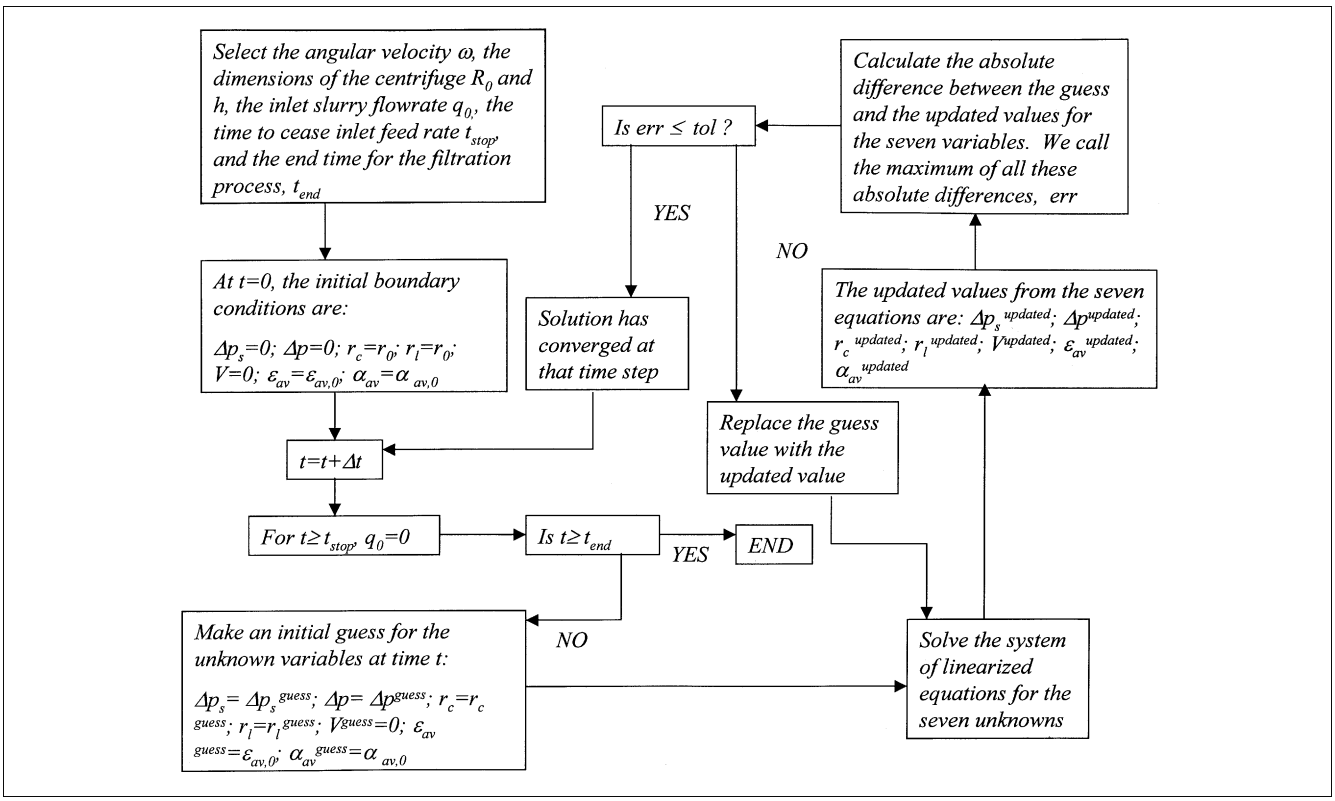

Figure 2a. Solution algorithm for centrifugation model.

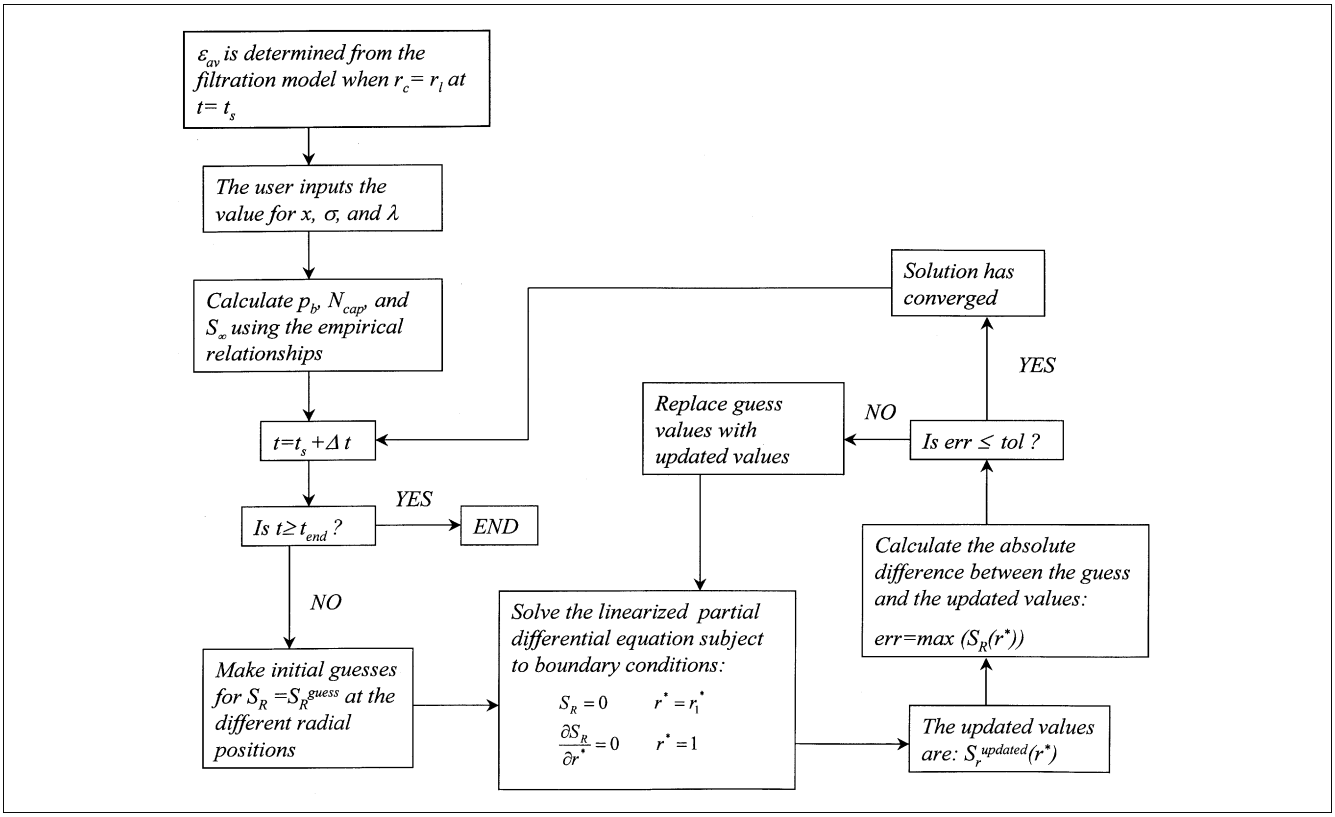

Figure 2b. Solution algorithm for deliquoring model.

liquid layer falls to the same level as the surface of the cake. Again, if the time exceeds or equals t_{end}, no more calculations are performed and the numerical algorithm stops here. The transient nonlinear second-order partial differential equation, given in Eq. 29 is first linearized (Chan and Cheh, 2001) and is subjected to the initial and boundary conditions given in Eqs. 34 and 35. The system of linear algebraic equations is discretized and is solved using the method of finite differences (Gerald and Wheatly, 1994). At the first time step $(t_s + \Delta t)$, the reduced saturation is assumed fully saturated for all radial positions as an initial guess $S_R^{guess}(r^*)$. After the first iteration, the updated values from solving the system of algebraic equations at the different positions yield $S_R^{updated}(r^*)$. If the absolute difference between the updated and the guess values is greater than an error tolerance of 10^{-8}, then the guess values are replaced with the updated values. The iterative process is repeated again until the error tolerance is met. The solution has converged when the set tolerance is satisfied and the new time is incremented by Δt. The same iterative process discussed above is then repeated at the next incremental time step. Figure 2b summarizes the iterative algorithm used to solve the partial differential equation.

Experimental Studies

Experimental determination of the cake resistance.

Due to the proprietary nature of the compound used in our investigation, the chemical structure of this entity is not disclosed. It has a molecular weight of approximately 345 gm $\cdot mol^{-1}$ and is referred to as "Compound A" in this discussion. The compressibility of the cake for Compound A is determined by performing a series of constant pressure experiments on a SS316L BHS Werk Sonthofen leaf filter (I.D. 5.0 cm). The experimental setup of the leaf filter to the pressure cylinder is shown in Figure 3. The type of filter medium used in all these filtration tests is Style SP-721—polypropylene (Shaffer Products Inc.) with a rating of 2–5 μm (nomial). A portion of the filter medium is cut from a slightly larger polypropylene cloth with a slightly larger diameter of ca. 5.2 cm to prevent any leaks or tunneling through the corners of the filter. The filter piece is immersed and is soaked in 190 proof ethanol for at least 5 min. The piece of wet filter medium is placed snuggly on top of the metal mesh of the filter. The position of the medium is adjusted so that the surface of the metal mesh is completely covered so that a small section of approximately 0.1 cm is wetted against the filter housing.

Before pouring the well-mixed slurry of Compound A into the filter, the bottom valve of the filter is set to the closed position. Approximately 200 cm^3 of the suspended feed solution (containing compound A in 190 proof ethanol) are used for each of these constant pressure tests. The top piece of the leaf filter is fitted on top of the housing and tightened manually. A pressure regulator with a maximum range of $6.89 \cdot (10)^5$ $N \cdot m^{-2}$ is connected to the outlet of a nitrogen cylinder and into the head of the filter. The pressure regulator is manually adjusted such that the pressure reading on the top piece of the leaf filter gives the desired set point.

At the instant the bottom valve of the leaf filter is switched to the open position, the time is set to zero when the first drop of filtrate lands on the graduated cylinder. The filtrate volume is collected in a graduated cylinder and data measurements are recorded in five-second intervals. Table 1 shows a summary of the slurry concentration used in each of the four tests.

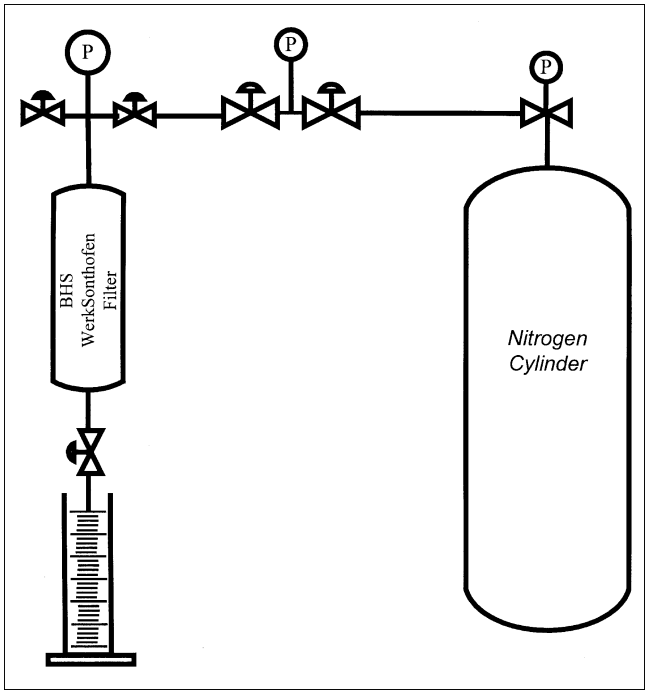

Figure 3. Experimental setup of leaf filter to the nitrogen cylinder.

For each experiment, the filtrate volume is plotted as a function of time and is found to follow the parabolic relationship (Lu, et al., 1998; Tiller et al., 1992) shown below

$$t = \frac{\alpha_{av}\mu c}{2\Delta p A^2}V^2 + \frac{\mu R_m}{\Delta p A}V \tag{48}$$

where

$$A = \pi r_0^2 \tag{49}$$

At each constant pressure, a second-order polynomial is used to fit the experimental data in order to obtain both the cake and medium resistance. A typical second-order polynomial curve at an applied pressure of $2.76 \cdot (10)^5$ $N \cdot m^{-2}$ is shown in Figure 4. A summary of the results at four different applied pressures is shown in Table 2. The compressibility of

Table 1. Calculated Slurry Concentrations Used in the Four Experiments

ΔP ($N \cdot m^{-2}$)	c (kg of Dry Solid/ m^3 of Filtrate Collected)
1.3×10^5	171
2.76×10^5	173
4.14×10^5	174
5.52×10^5	175

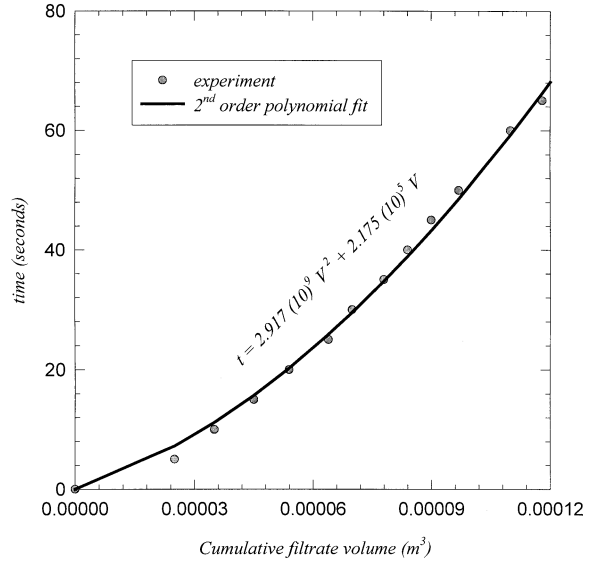

Figure 4. Cumulative filtrate volume versus time at constant pressure of 2.76×10^5 N·m^{-2}.

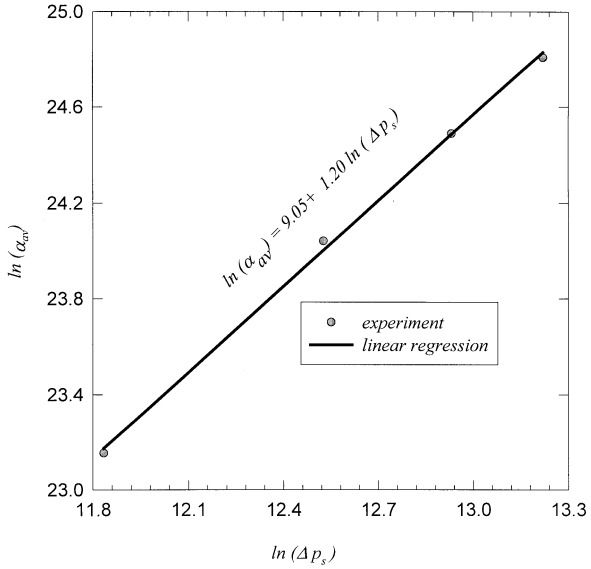

Figure 5. Natural logarithm of cake resistance versus logarithm of applied pressure.
Units of Δp_s is N·m^{-2}; units of α_{av} is Kf·m^{-1}.

the cake is determined from the slope of a plot of the natural logarithm of the cake resistance vs. the natural logarithm of the applied pressure, shown by the relationship below

$$\ln \alpha_{av} = \ln \alpha_0 + n_1 \ln(\Delta p_s) \tag{50}$$

From a plot of this relationship shown in Figure 5, the compressibility of the cake is determined to be 1.2, indicating the highly compressive nature of the cake, and the value of the pre-exponential coefficient is found to be 8,520. Based on this analysis, the following empirical relationship, correlating the cake resistance as a function of the compressive pressure, is obtained

$$\alpha_{av} = 8520(\Delta p_s)^{1.2} \tag{51}$$

In this expression, the compressive pressure Δp_s is expressed in units of N·m^{-2} in order to obtain a cake resistance in units of $m\cdot kg^{-1}$.

From a plot of the natural logarithm of the porosity vs. the natural logarithm of the applied pressure, the values of the constants ϵ_0 and n_2 are determined similar to the cake resistance analysis discussed previously. From leaf filter tests performed under various conditions, the wet cakes are dried at 28–30°C under vacuum until a loss on drying (LOD) value of less than 0.1% is obtained. It is possible that the pore structure of the dry powder may have been different from the wet cakes when dried under vacuum leading to sources of error in the determination of the average porosity. In this analysis, a key assumption is that the porosity of the dry powder is not much different than that of the wet cake.

Table 2. Summary of the Cake and Medium Resistances

Δp ($N\cdot m^{-2}$)	α_{av} ($m\cdot kg^{-1}$)	R_m (m^{-1})
1.38×10^5	1.14×10^{10}	5.76×10^{10}
2.76×10^5	2.76×10^{10}	9.05×10^{10}
4.14×10^5	4.32×10^{10}	1.3×10^{11}
5.52×10^5	5.94×10^{10}	1.8×10^{11}

At each applied pressure, the dried powder is mixed thoroughly by mechanically shaking it in a glass jar for at least three minutes until a homogeneous mixture is obtained. A minimum of at least three bulk density measurements, where samples are independently taken in different regions of the jar, is performed to ensure that an average porosity was measured. The bulk density of the powder ρ_b is found by the tapping method (ASTM, 1995). The true density of the powder ρ_t is measured by the displacement of the helium gas (ASTM, 1997) using an AccuPyc 1330 Pycnometer and is found to have a value of 1.09 g/cm^3. From a determination of the true and bulk density of the powder, the average porosity of the powder at each applied pressure is calculated by the relationship shown below

$$\epsilon_{av} = 1 - \frac{\rho_b}{\rho_t} \tag{52}$$

With this method, the average experimental porosities, with a maximum standard deviation of 0.03, are shown in Figure 6 at each applied pressure. An alternative wet cake method is also used to verify the measurement of average porosity, using the equation shown below

$$\epsilon_{av} = 1 - \frac{m_s}{LA\rho_t} \tag{53}$$

where m_s is the mass of the dry solid, A is the cross sectional surface area of the leaf filter, and L is the thickness of the wet cake. Fair agreement is found between the average porosity measurements using two different methods. From a linear regression analysis, the values of ϵ_0 and n_2 are determined to be 0.90 and 0.03, respectively. Both relations 10 and 11 are valid when the value of the compressive pressure is

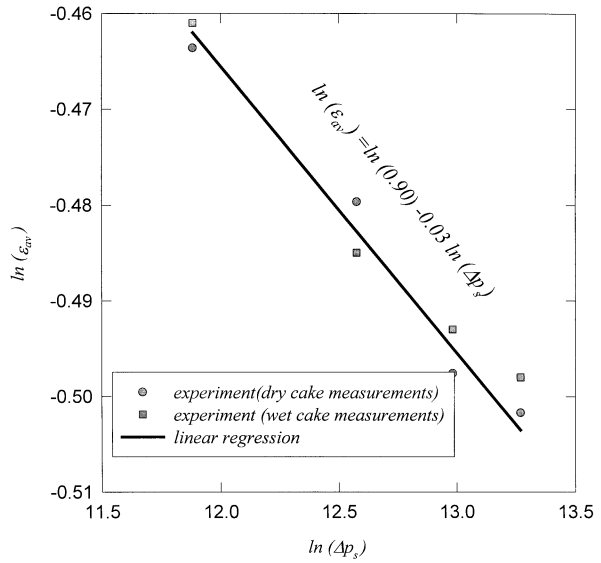

Figure 6. Natural logarithm of porosity vs. natural logarithm of applied pressure.

Units of Δp_s is $N \cdot m^{-2}$.

greater than 20 $N \cdot m^{-2}$. Below this pressure, both the cake compressibility and porosity are constant values, as defined previously in Eq. 45a and 46a. An important assumption is that the experimentally determined values in the power law expressions at these high compressive pressures can be extrapolated to the low compressive pressures used in the centrifugation experiments.

The mean geometric diameter, using the volume distribution method, is measured by dispersing the dry solid in an Aerosizer (Amherst Process Instruments, Inc.). Table 3 shows the percent volume distribution tabulated against the different ranges for the geometric diameter. The mean geometric diameters, corresponding to applied pressures of $1.38 \cdot (10)^5$, $2.76 \cdot (10)^5$, $4.14 \cdot (10^5)$, and $5.52 \cdot (10)^5$ $N \cdot m^{-2}$, are calculated to be 21.6, 16.7, 13.3 , 10.04 μm, respectively. The mean geometric diameter is found to decrease with an increase in the applied pressure, due to fracturing of the crystals at the higher compressive forces.

Centrifugation experiments

The following is a list of the physicochemical parameters used in the prediction of the filtration performance in a basket centrifuge: $\mu = 0.001$ Pa·s, $\rho_\ell = 810$ kg·m^{-3}, $V_s = 0.35$, $\sigma = 23$ dynes·cm^{-1}, and $c = 171$ kg·m^{-3}. Based on the experimental leaf filtration tests, a medium resistance value of $2 \cdot 10^{11}$m^{-1} is used in the centrifugation model. A gear pump (Barnant Company, Model No: 900-374 180/3600 RPM) is used to transfer the slurry from a well-agitated Erlenmeyer flask, through a 3/8 in Teflon tube, to the rotor basket centrifuge (International Equipment Centrifuge, Centra-CF) operating at a constant angular velocity. The dimensions of the height and the inner diameter of the horizontal basket centrifuge are 5.5 cm and 13 cm, respectively. The angular rotation speed for this centrifuge is from 1045 to 419 rad·s^{-1}, corresponding to a g-force of 72 to 1,470, respectively. The assumption, that the presence of a slurry layer is absent in the basket, can be made by calculating the centrifugal sedimentation velocity (McCabe and Smith, 1967; Perry, 1984)

$$v_s = \frac{\omega^2 r(\rho_t - \rho_\ell) x^2}{18\mu} \tag{54}$$

In the range of rotation speeds studied, the sedimentation velocities range from 26.8 cm·s^{-1} to 412 cm·s^{-1}, assuming an average particle diameter of 50 μm. On this scale, the approximate time for the separation of both a liquid and a cake layer is calculated to range from 0.016 to 0.24 s. This empirical relationship shows that better agreement between experiment and theory would occur at the high rotation speeds.

Table 3. Mean Geometric Diameter Calculated Based on Volume Distribution

Pressure ($N \cdot m^{-2}$)	Diameter Range (ωmm)	Percentage (%)	Mean Geometric Diameter (μm)
	less than 5.6	5	
	5.6 to 13.1	15	
	13.1 to 19.6	15	
$1.38 \times (10^5)$	19.6 to 23.6	10	21.6
	23.6 to 27.6	10	
	27.6 to 33.9	15	
	33.9 to 39.8	15	
	39.8 to 44.9	10	
	greater than 44.9	5	
	less than 3.1	5	
	3.1 to 8.6	15	
	8.6 to 14.4	15	
	14.4 to 20.2	10	
$2.76 \times (10)^5$	20.2 to 25.6	10	16.7
	25.6 to 30.2	15	
	30.2 to 34.8	15	
	34.8 to 39.6	10	
	greater than 39.6	5	
	less than 2.2	5	
	2.2 to 6.6	15	
	6.6 to 10.8	15	
	10.8 to 15.6	10	
$4.14 \times (10)^5$	15.6 to 20.0	10	13.3
	20.0 to 24.9	15	
	24.9 to 30.1	15	
	30.1 to 34.6	10	
	greater than 34.6	5	
	less than 1.6	5	
	1.6 to 4.6	15	
	4.6 to 7.8	15	
$5.52 \times (10)^5$	11.4 to 15.8	10	10.04
	15.8 to 20.0	10	
	20.0 to 23.6	15	
	23.6 to 27.2	15	
	27.2 to 31.8	10	
	greater than 31.8	5	

Results and Discussion

Figure 7 shows a series of curves at different angular velocities where the cumulative filtrate volume is plotted as a function of time at a constant inlet feed rate of $4.5 * 10^{-6}$ m$^3 \cdot$s^{-1}. In this figure, the different shaped polygons represent the experimental data, while the solid lines represent

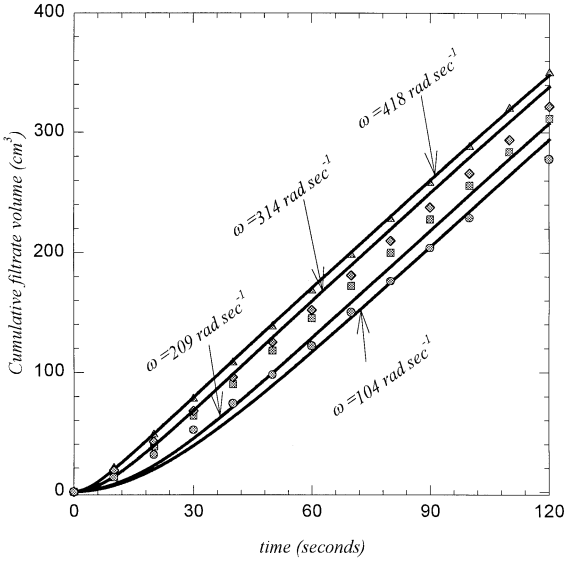

Figure 7. Cumulative filtrate volume vs. time at constant feed rate of $q_0 = 4.5 \times 10^{-6}$ m$^3 \cdot$ s^{-1}.

Shaded polygons represent experimental data, while lines represent model.

simulation results based on the centrifugation model. At a given instant, the figure shows that more filtrate volume is collected at higher angular velocities because the centrifugal force is greater than the combined resistive forces of both the cake and medium.

Plots of the volumetric flow rate of the filtrate vs. time at different angular velocities are shown in Figure 8, corresponding to the filtration performance curves in Figure 7. By definition, the volumetric flow rate is defined as

$$q = \frac{dV}{dt} = \lim_{t_1 \to t_2} \frac{V(t_2) - V(t_1)}{t_2 - t_1} \tag{55}$$

In Figure 8 the experimental flow rate is estimated by taking the difference between the filtrate volumes divided by the time difference

$$q_{\text{expt}} \approx \frac{V(t_2) - V(t_1)}{t_2 - t_1} \tag{56}$$

In this study, the experimental data are collected in equal time intervals of approximately 10 s apart. Because only a discrete number of experimental data points are collected during the filtration process, there are definitely some errors introduced by using this approximation because $(t_2 - t_1)$ approaches a finite value instead of zero. At angular rotation speeds of 104 and 209 rad s^{-1}, Figure 8 shows that the experimental flow rate is higher than that predicted by the theoretical model during the initial startup. This is because most of the resistance felt by the filtrate is that due primarily to the filter medium when no cake is deposited. This is shown in Figure 8 during the initial period when the filtrate flow increases steeply as a function of time, because the centrifugal

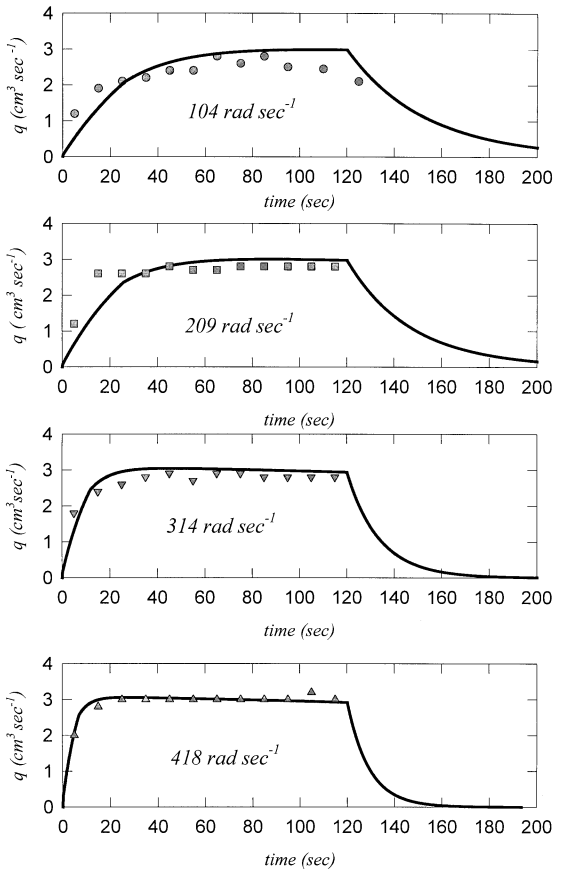

Figure 8. Filtrate flow rate vs. time at different angular rotation speeds.

Shaded Polygons represent experiments, while lines represent model.

force on the fluid is much greater than the sum of the resistive forces contributed by both the cake and the medium. After a sufficient buildup of cake, the resistive forces of the cake and medium become equal to and greater than the centrifugal force on the fluid, leading to a plateau effect. Only experimental data during the first 120 s are shown corresponding to a constant inlet feed rate. For filtration times exceeding 120 s, the inlet feed is set to zero. As the liquid drains and falls below the surface of the cake, the deliquoring model is used to calculate the flow rate of the filtrate. Figure 8 show that the filtrate flow rate decreases with increasing time and the rate is greater at higher angular rotation speeds, because higher centrifugal forces are experienced by the filtrate trapped inside the cake.

Figure 9 shows a plot of the cumulative filtrate volume vs. time for different inlet feed rates at a constant angular velocity of 209 rad$\cdot$s^{-1}. At a given time, the plot that shows more filtrate volume is collected at larger inlet feed rates. This is attributed to the presence of a thicker liquid layer above the surface of the cake at higher inlet feed rates, leading to a larger hydraulic pressure drop. The corresponding volumetric flow rate of the filtrate vs. time is shown in Figure 10 at two different q_0. Again, a similar trend to Figure 8 is shown here in Figure 10.

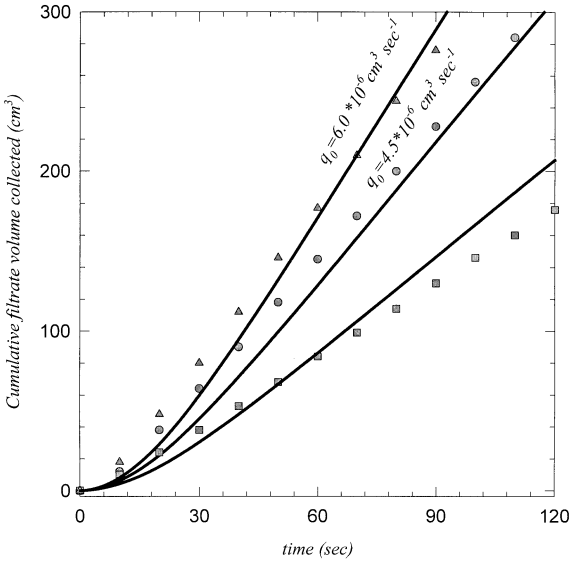

Figure 9. Cumulative filtrate volume vs. time at constant angular rotation speed of 209 rad s^{-1} ($R_m = 2 \times 10^{11}$ m^{-1}).

Shaded polygons represent experiments, while lines represent model.

The average error E_{av} is defined by the relationship shown below

$$E_{av} = \frac{1}{N} \sum_{i=1}^{N} \left| \frac{V_{\text{expt}} V(t_i) - V_{theo}(t_i)}{V_{\text{expt}}(t_i)} \right| \qquad (57)$$

where $V_{\text{expt}}(t_i)$ is the cumulative experimental filtrate volume collected at t_i, $V_{theo}(t_i)$ is the cumulative theoretical filtrate volume collected at t_i, and N is the total number of experimental data points collected between t_1 and t_N, inclusive. A summary of the average error between both theory and experiment is shown in Table 4.

Table 4. Calculated Average Error

Inlet Feed Rate ($m^3 \cdot s^{-1}$)	Angular speed ($rad \cdot s^{-1}$)	E_{avg}
4.5×10^{-6}	104	17.6%
4.5×10^{-6}	209	13.0%
4.5×10^{-6}	314	5.3%
4.5×10^{-6}	419	2.8%
3.0×10^{-6}	209	14.0%
6.0×10^{-6}	209	12.2%

The table shows that the average error decreases as the rotation speed increases at a constant inlet feed rate of $4.5 \cdot 10^{-6} m^3 \cdot s^{-1}$. With an angular velocity of 209 $rad \cdot s^{-1}$, the average error remains unchanged as the volumetric flow rate increases. The instantaneous formation of both a liquid and a cake layer as the slurry deposits on the basket is a better assumption at the higher rotation speeds. Better agreement between theory and experiment is found at the higher speeds because of the larger sedimentation velocities of the crystals.

A plot of r_c and r_ℓ vs. time is shown in Figure 11 at an inlet feed rate of $4.5 \cdot 10^{-6}$ $m^3 \cdot s^{-1}$ and a rotation speed of 105 $rad \cdot s^{-1}$. At $t = 0$, both the liquid layer and the cake thickness originate from the radius of the centrifuge. At the start of the filtration process, most of the resistance experienced by the filtrate is that due primarily to the filter medium, so that only a small liquid layer lies above the cake. After sufficient buildup of cake, the resistance of the cake is much greater than the resistance of the medium so that the liquid layer above the cake $r_c - r_\ell$ increases with time. In order to keep the centrifuge from flooding, the inlet feed is arbitrarily chosen to cease after 120 s. Once the inlet flow stops, Figure

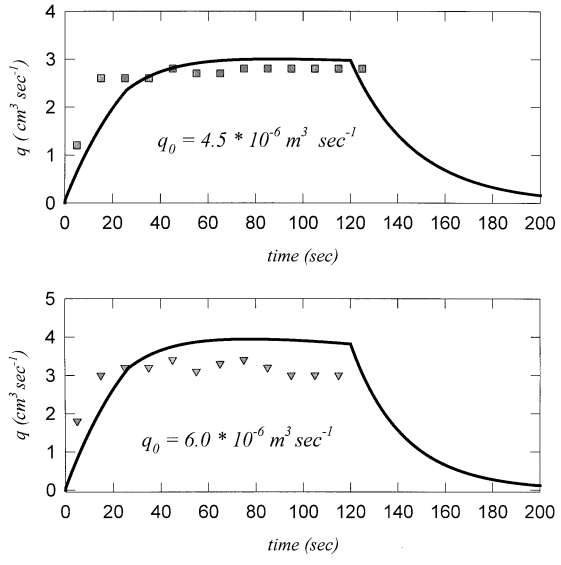

Figure 10. Filtrate flow rate vs. time at different inlet feed rates.

Shaded polygons represent experiments, while lines represent model.

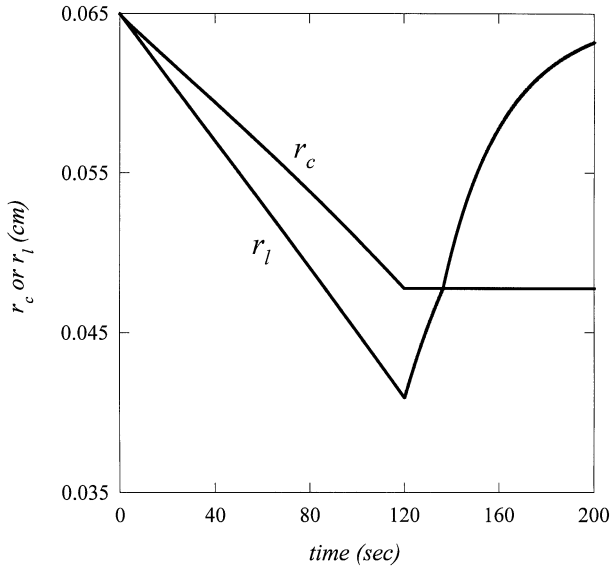

Figure 11. Cake radius or liquid radius vs. time.

$q_0 = 4.5 \times 10^{-6}$ m^3 s^{-1}, $\omega = 105$ $rad \cdot s^{-1}$

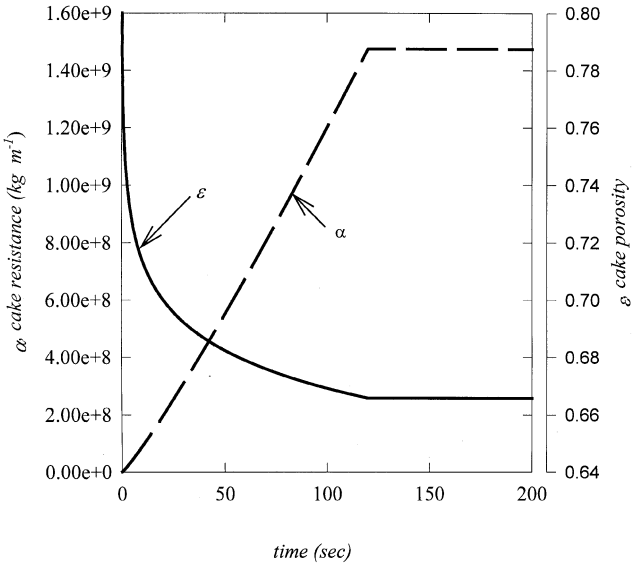

Figure 12. Cake resistance /cake porosity vs. time.

$q_0 = 4.5 \times 10^{-6}$ m^3 s^{-1} for $t < 120$ s and $q_0 = 0$ for $t > 120$ s, $\omega = 105$ rad·s^{-1}

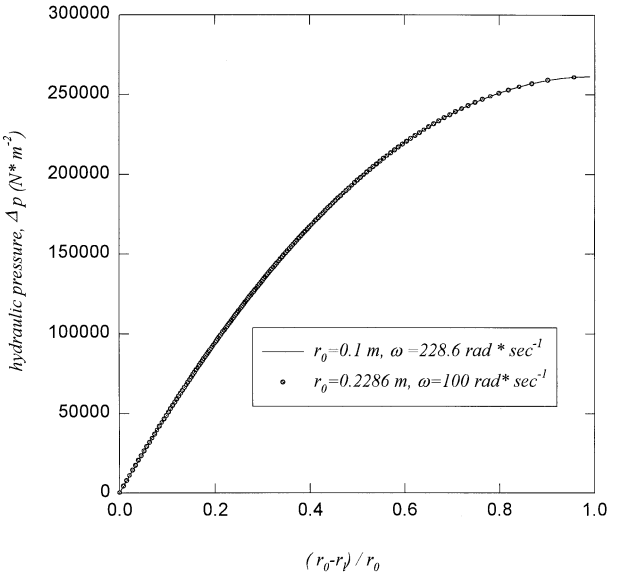

Figure 14. Hydraulic pressure vs. fraction of the liquid layer.

11 shows the liquid layer above the cake continues to decrease at a linear rate up to the cake layer. Below the surface of the cake, the liquid continues to drain but at a slower rate due to a smaller drop in the hydraulic pressure.

This model can also be extended for applications where the inlet feed rate can be regulated. By adjusting the inlet feed, an optimal process can be designed where only a small liquid layer is allowed to lie above the surface of the cake at any time during the buildup.

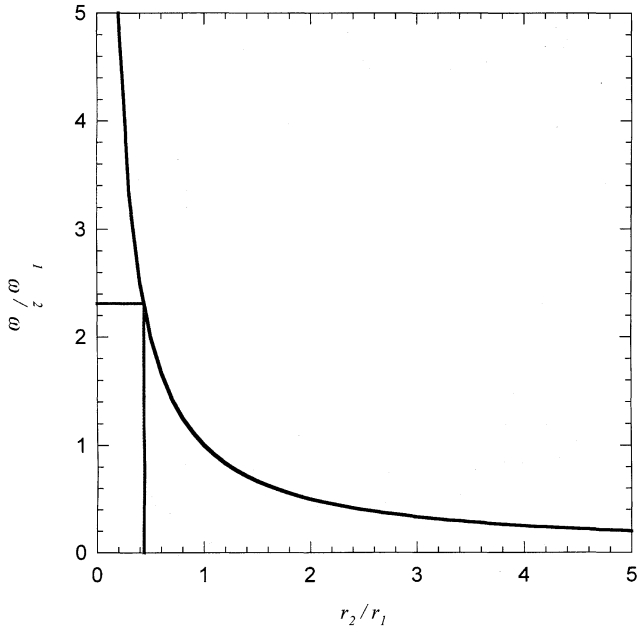

Figure 13. Universal curve for correlating two different sized centrifuges with the same dynamic performance.

Figure 12 shows a plot of the cake porosity/cake resistance vs. time at an inlet feed rate of $4.5 \cdot 10^{-6}$ m$^3 \cdot$s^{-1} (for time values less than or equal to 120 s) and an angular velocity of 209 rad·s^{-1}. At a constant inlet feed rate, the cake resistance varies linearly with time because the compressive pressure is raised to the power of 1.2. The porosity decreases from 0.82 to 0.68 over a short time interval of about 50 s, showing the sensitivity of the compressive pressure raised to the power of negative 0.03. When the inlet feed rate ceases, both the cake resistance and the porosity remains constant.

Figure 13 shows a universal curve for a basket centrifuge where the cake performance on two different scales is dynamically similar provided that the intrinsic relation $\omega_1 r_1 = \omega_2 r_2$ (see derivation in Appendix A) is satisfied. Similar dynamic performance occurs when the same hydraulic pressure is experienced by the cake on two different centrifuges at the same ratio of the liquid layer thickness to the centrifuge radius. ω_1 and r_1 and represent, respectively, the angular velocity and the inner radius of the basket for centrifuge C1. Similarly, the respective angular velocity and the inner radius of the basket for centrifuge C2 are denoted by ω_2 and r_2. An example is discussed below to demonstrate the practicality of this curve.

Let us assume centrifuge C1, with a radius of r_1, is operating at an angular velocity of ω_1. In order to obtain the same dynamic performance on centrifuge C2 with a radius of r_2, the value of r_2/r_1 is located on the abscissa and a vertical line is drawn until it intersects the curve. At the point of intersection for both the curve and the line, a horizontal line is drawn until it intersects the value of the ω_2/ω_1 on the ordinate. From this value, the angular velocity can then be evaluated. This calculated angular rotation speed is a conservative value such that the forces experienced on centrifuge C2 is equivalent and no greater than the forces exerted on centrifuge C1.

An example demonstrating the practicality of this universal curve in scaling centrifuges is shown in Figure 14. The figure

assumes a constant inlet feed rate and is plotted until the centrifuge is completely flooded. Simulation results showed that the same hydraulic pressure is experienced by the cake at the same ratio of the liquid layer thickness to the centrifuge radius on two different scales by application of this scaling relation.

Conclusions

A 1-D mathematical model based on Darcy's law and conservation of mass was presented in this article for the filtration prediction in a basket centrifuge. The power law relationships for both the resistance and the porosity of the cake were adopted in this study. Both the porosity and resistance of the cake were assumed to be constant throughout the cake at any instant in time. The system of nonlinear equations derived from the model was solved numerically by using an iterative algorithm. "Compound A" was used as the powder of interest to verify the theoretical model. Fair agreement was found between theoretical and experimental filtration performance curves. For the particular compound and the range of conditions, both theory and experiment showed similar trends during the initial startup when the filtrate flow rate increased as a function of time and the liquid layer was predicted to be above the surface of the cake at a constant inlet feed rate. An intrinsic relation had also been developed to use small-scale lab data, in conjunction with the model, to select a rotation speed for large-scale equipment so that cake performance was dynamically similar on both scales. Simulation results showed the validity of this scaling relation on two different scales. For the case when the inlet feed ceased and the liquid layer fell below the surface of the cake, the cake deliquoring model proposed by Wakeman and Vince was adopted in the numerical model.

Acknowledgments

The authors thank Dr. Margaret Peel (Crystallization Laboratories) for preparing the slurry used in these filtration tests and William Merkl (Process Safety and Evaluation Laboratories) for his assistance in running and interpreting the Aerosizer results. Special thanks is also given to Andrew Schafranek (Stevens Institute of Technology, Hoboken, NJ), a summer intern, for his assistance in these experiments. I would also like to acknowledge Dr. Richard Mueller and Katherine Wu for their careful review of this manuscript.

Notation

A_{av} = arithmetic mean surface area of the cake, m^2
A_{lm} = logarithmic mean surface area of the cake, m^2
A_0 = surface area of the basket centrifuge, m^2
A = cross sectional area of the leaf filter, m^2
c = concentration of slurry, weight of dry solids divided by the volume of filtrate collected, $kg \cdot m^{-3}$
E_{av} = average error
h = height of the centrifuge basket, m
h_1 = basket height in centrifuge C1, m
h_2 = basket height in centrifuge C2, m
k = permeability of the saturated medium, m^2
$k_{r\ell}$ = relative permeability of the cake to the liquid phase
L = thickness of the wet cake, m
m_s = mass of the dry solid, g
N_{cap} = capillary number
N = total number of experimental data points collected between time t_1 and t_N
n_1 = cake compressibility
n_2 = porosity compressibility
p_b = minimum pressure needed to initiate displacement of liquid in cake $(N \cdot m^{-2})$
p_c = capillary pressure $(N \cdot m^{-2})$
Δp = hydraulic pressure $(N \cdot m^{-2})$
Δp_i^{guess} = guess value of the hydraulic pressure at time $t_i (N \cdot m^{-2})$
$\Delta p_i^{updated}$ = updated value of the hydraulic pressure at time t_i $(N \cdot m^{-2})$
$\Delta p_{s,0}$ = minimum compressive pressure of the cake, $N \cdot m^{-2}$
Δp_s = compressive pressure of the cake, $N \cdot m^{-2}$
$\Delta p_{s,i}^{guess}$ = guess value for the compressive pressure of the cake at time t_i, $N \cdot m^{-2}$
$\Delta p_{s,i}^{updated}$ = updated value for the compressive pressure of the cake at time t_i, $N \cdot m^{-2}$
q_{expt} = experimental volumetric flow rate, $m^3 \cdot s^{-1}$
q = volumetric flow rate of the filtrate, $m^3 \cdot s^{-1}$
q_1 = volumetric flow rate of the filtrate in centrifuge C1, $m^3 \cdot s^{-1}$
q_2 = volumetric flow rate of the filtrate in centrifuge C2, $m^3 \cdot s^{-1}$
q_0 = volumetric flow rate of the slurry feed rate, $m^2 \cdot s^{-1}$
R_m = resistance of the filter medium, m^{-1}
r_0 = radius of the centrifuge basket, m
r_1 = basket radius in centrifuge C1, m
r_2 = basket radius in centrifuge C2, m
r_c = distance from the center to the surface of the cake in a centrifuge, m
$r_{c,i}^{guess}$ = guess value of the radius from the center of the basket to the surface of the cake at time t_i, m
$r_{c,i}^{updated}$ = updated value of the radius from the center of the basket to the surface of the cake at time t_i, m
r_ℓ = radius from the center of the basket to the surface of the liquid front, m
$r_{\ell,i}^{guess}$ = guess value of the radius from the center of the basket to the surface of the liquid front at time t_i, m
$r_{\ell,i}^{updated}$ = updated value of the radius from the center of the basket to the surface of the liquid front at time t_i, m
S_R = reduced saturation, $(S - S_\infty)/(1 - S_\infty)$
S_∞ = saturation at which liquid flow ceases
$S_{R,avg}$ = average reduced saturation
$S_R^{updated}$ = updated value of the reduced saturation
S_R^{guess} = guess value of the reduced saturation
Δt = time increment used in the control volume method, s
t = time, s
t_s = instant when the liquid layer falls to same level as the surface of the cake, s
t_{stop} = time when the inlet feed ceases, s
t_{end} = end time when the numerical algorithm stops, s
V = cumulative filtrate volume, m^3
V_i^{guess} = guess value of the cumulative filtrate volume at time t_i, m^3
$V_i^{updated}$ = updated value of the cumulative filtrate volume at time t_i, m^3
$V_{expt}(t_i)$ = cumulative experimental filtrate volume at time t_i m^3
$V_{theor}(t_i)$ = cumulative theoretical filtrate volume at time $t_i (m^3)$
V_s = solid volume fraction of the inlet slurry
V_{pore} = void volume in the cake, m^3
V_ℓ = liquid volume in the cake, m^3
x = mean particle size, μm

Greek letters

α_{av} = average cake resistance $(m \cdot kg^{-1})$
$\alpha_{av,i}^{guess}$ = guess value of the average cake resistance at time t_i $(m \cdot kg^{-1})$
$\alpha_{av,i}^{updated}$ = updated value of the average cake resistance at time, t_i $(m \cdot kg^{-1})$
α_0 = pre-exponential value in the constitutive cake resistance expression
ϵ_{av} = average cake porosity
$\epsilon_{av,i}^{guess}$ = guess value of the average cake porosity at time t_i
$\epsilon_{av,i}^{updated}$ = updated value of the average cake porosity at time t_i
ϵ_0 = pre exponential value in the constitutive porosity expression

λ = pores size index
ρ_ℓ = liquid density of the filtrate, $kg \cdot m^{-3}$
ρ_t = true density of the dried solid, $kg \cdot m^{-3}$
ρ_b = bulk density of the dried solid, $kg \cdot m^{-3}$
σ = liquid surface tension, $N \cdot m^{-1}$
μ = viscosity of the filtrate, $Pa \cdot s$
v_s = centrifugal sedimentation velocity, $cm \cdot s^{-1}$
ω = angular velocity of the centrifuge, $rad \cdot s^{-1}$
ω_1 = angular velocity in centrifuge C1, $rad \cdot s^{-1}$
ω_2 = angular velocity in centrifuge C2, $rad \cdot s^{-1}$

Literature Cited

American Society for Testing and Materials, *Standard Test Method for Real Density of Calcined Petroleum Coke by Helium Pycnometer*, ASTM, D2638-91 (1997).

American Society for Testing and Materials, *Standard Test Method for Determination of Tap Density of Metallic Powders and Compounds*, ASTM, B527-93 (1995).

Chan, S. H., and H. Y. Cheh, "Modelling of Through-Hole Electrodeposition. Part I: Effect of Electrical Migration," *J. Appl. Electrochem.*, **31**, 605 (2001).

Fournet, F., J. P. Klein, G. Baluais, J. F. Remy, J. A. Dodds, and D. Leclerc, "Laboratory Tests and Methodology for the Design and Centrifugal Filtration-Washing-Dewatering Cycles," *Filtration & Sep.*, **29**(3), 254 (1992).

Gerald, C. F., and P. O. Wheatly, *Applied Numerical Analysis, 5th Edition*, Addison-Wesley Publishing, MA (1994).

Lu, W. M., Y. P. Huang, and K. J. Hwang, "Dynamic Analysis of Constant Rate Filtration Data," *J. Chem. Eng. Jpn.*, **31**, 969 (1998).

McCabe, W. L., and J. C. Smith, *Unit Operations of Chemical Engineering, 2nd Edition*, McGraw-Hill, New York (1967).

Perry, R. H., *Perry's Chemical Engineers' Handbook, 6th Edition*, McGraw-Hill, New York (1984).

Sambuichi, M., H. Nakakura, K. Osasa, and F. M. Tiller, "Theory of Batchwise Centrifugal Filtration," *AIChE J.*, **33**, 109 (1987).

Tiller, F., and W. J. Leu, "Basic Data Fitting in Filtration," *J. of Chinese Inst. of Chem. Eng.*, **11**, 61 (1980).

Tiller, F. M., and N. B. Hsyung, "Relative Performance of Filters and Centrifuges with Respect to Average Cake Porosity," *Adv. Filtr. Sep. Technol.*, **3**, p. 262 (1991).

Tiller, F., D. Cong, and N. B. Hsyung, "New Revolving Laboratory Filter," *Adv. Filtr. Sep. Technol.*, **6**, 45 (1992).

Wakeman, R. J., "Modelling Slurry Dewatering and Cake Growth in Filtering Centrifuges," *Filtration and Sep.*, **31**(1), 75 (1994).

Wakeman, R. J., and E. S. Tarleton, *Filtration: Equipment Selection, Modelling and Process Simulation*, 1st Edition. Elsevier Science Ltd., Oxford, U.K. (1999).

Wakeman, R. J., and A. Vince, "Engineering Model for the Kinetics of Drainage for Centrifuge Cakes," *Chem. Eng. Res. Des.*, **64**(2), 104 (1986).

Wakeman, R. J., "Vacuum Dewatering and Residual Saturation of Incompressible Filter Cakes," *Int. J. Miner. Process.*, **5**, 193 (1976).

Wakeman, R. J., and A. Rushton, "Dewatering Properties of Particulate Beds," *J. Powder Bulk Solids Technol.*, **1**, 64 (1977).

Appendix A

Let us assume we have centrifuge filters of two different scales, denoted by centrifuge C_1 and centrifuge C_2. Centrifuge C_1 has dimensions of r_1 and h_1, while centrifuge C_2 has dimensions of r_2 and h_2, corresponding to the radius and heights, respectively.

It is assumed that the same type of slurry, with identical physicochemical properties, is fed to centrifuge at such a flow rate (q_1 for centrifuge C_1 and q_2 for centrifuge C_2) so that a liquid layer always exists above the cake.

For centrifuge C_1, the hydraulic pressure drop Δp_1 across the cake and liquid layers is

$$\Delta p_1 = \frac{\rho_\ell \omega_1^2}{2}\left(r_1^2 - r_{\ell,1}^2\right) \tag{A1}$$

where $r_{\ell,1}$ is the distance from the center to the surface of the liquid layer and ω_1 is the rotation speed of the centrifuge.

Similarly, for centrifuge C_2, the hydraulic pressure drop Δp_2 across the cake and the liquid layers is

$$\Delta p_2 = \frac{\rho_\ell \omega_2^2}{2}\left(r_2^2 - r_{\ell,2}^2\right) \tag{A2}$$

The hydraulic pressures in Eqs. A1 and A2 are set equal to each other

$$\frac{\rho_\ell \omega_1^2}{2}\left(r_1^2 - r_{\ell,1}^2\right) = \frac{\rho_\ell \omega_2^2}{2}\left(r_2^2 - r_{\ell,2}^2\right) \tag{A3}$$

By factoring r_1^2 and r_2^2, respectively, on the lefthand and righthand sides of the parentheses and reducing to simplest terms, the following equation was obtained

$$\omega_1^2 r_1^2\left(1 - \frac{r_{\ell,1}^2}{r_1^2}\right) = \omega_2^2 r_2^2\left(1 - \frac{r_{\ell,2}^2}{r_2^2}\right) \tag{A4}$$

We set the expression inside the parentheses equal to each other to obtain

$$\left(1 - \frac{r_{\ell,1}^2}{r_1^2}\right) = \left(1 - \frac{r_{\ell,2}^2}{r_2^2}\right) \tag{A5}$$

In order for the expression in Eq. A5 to be true, the following relationship must also be satisfied

$$\left(1 - \frac{r_{\ell,1}}{r_1}\right) = \left(1 - \frac{r_{\ell,2}}{r_2}\right) \tag{A6}$$

The expression without any parentheses in Eq. A4 must also be set equal to each other

$$\omega_1^2 r_1^2 = \omega_2^2 r_2^2 \tag{A7}$$

By taking the square root on both sides of Eq. A7 we obtain

$$\omega_1 r_1 = \omega_2 r_2 \tag{A8}$$

which is the intrinsic relationship where similar dynamic performance is exhibited on centrifuges of two different scales.

Manuscript received Sept. 6, 2001, and revision received Oct. 21, 2002.